Frontier Orbital Consistent Quantum Capping Potential (FOC-QCP) for Bulky Ligand of Transition Metal Complexes

Yu-ya Ohnishi,[†] Yoshihide Nakao,[†] Hirofumi Sato,[†] and Shigeyoshi Sakaki*[,†,‡]

Department of Molecular Engineering, Graduate School of Engineering, Kyoto University, Nishikyo-ku, Kyoto 615-8510, Japan, and [‡]Fukui Institute for Fundamental Chemistry, Kyoto University, Nishihiraki-cho, Takano, Sakyo-ku, Kyoto 606-8103, Japan

Received: October 25, 2007; In Final Form: December 10, 2007

Chemically reasonable models of PR_3 (R = Me, Et, ^{i}Pr, and ^{t}Bu) were constructed to apply the post Hartree−Fock method to large transition metal complexes. In this model, R is replaced by the H atom including the frontier orbital consistent quantum capping potential (FOC-QCP) which reproduces the frontier orbital energy of PR_3. The steric effect is incorporated by the new procedure named steric repulsion correction (SRC). To examine the performance of this FOC-QCP method with the SRC, the activation barriers and reaction energies of the reductive elimination reactions of C_2H_6 and H_2 from $M(R^1)_2(PR^2_3)_2$ (M = Ni, Pd, or Pt; R^1 = Me for R^2 = Me, Et, or ^{i}Pr, or R^1 = H for R^2 = ^{t}Bu) were evaluated with the DFT[B3PW91], MP4(SDQ), and CCSD(T) methods. The FOC-QCP method reproduced well the DFT[B3PW91]- and MP4(SDQ)-calculated energy changes of the real complexes with PMe_3. For more bulky phosphine, the SRC is important to present correct energy change, in which the MP2 method presents reliable steric repulsion correction like the CCSD(T) method because the systems calculated in the SRC do not include a transition metal element. The monomerization energy of $[RhCl(P^iPr_3)_2]_2$ and the coordination energies of CO, H_2, N_2, and C_2H_4 with $[RhCl(P^iPr_3)_2]_2$ were theoretically calculated by the CCSD(T) method combined with the FOC-QCP and the SRC. The CCSD(T)-calculated energies agree well with the experimental ones, indicating the excellent performance of the combination of the FOC-QCP with the SRC. On the other hand, the DFT[B3PW91]-calculated energies of the real complexes considerably deviate from the experimental ones.

1. Introduction

In many computational studies of transition metal complexes, the DFT method is widely used nowadays. However, the DFT method tends to underestimate the binding energies of late-transition metal complexes with large π-conjugate systems.[1] Also, the DFT method does not describe correctly the dispersion interaction[2] which plays important role in the interaction between bulky ligand and bulky substrate. In such cases, post-Hartree−Fock (HF) methods should be employed. Møller−Plesset (MP) perturbation theory, the least expensive post-HF method, is usually applied to large system since its computational cost is reasonable. The MP method, however, often fails to describe the electronic structure of the first-row transition metal complex[3,4] since the electron correlation effect is considerably large and the HF wave function, which is used as a reference wave function of the MP method, is much different from exact wave function in the first-row transition metal complex. On the other hand, *ab initio* methods such as CCSD(T) (coupled cluster singles and doubles with noniterative evaluation of triples), CCSDT, and CASPT2 (complete active space with second-order perturbation theory) methods can present reliable results in most of the first-row transition metal complexes such as nickel[4] and chromium[5] complexes. However, they need considerably large computational cost.

Because of the large computational cost, various quantum mechanical/molecular mechanical (QM/MM) methods are widely used for the theoretical studies of large systems.[6] In the QM/MM method, a whole system is spatially divided into the chemically active region and the environment region.[7−9] The QM/MM method is becoming the standard technique to investigate proteins nowadays.[10] This method is also used to study solid catalysts[11] and transition metal complexes.[12,13]

However, the QM/MM method involves problems. Boundary problem is one of the major problems in the QM/MM methods, as is well-known, which is how to treat the connection between the QM and the MM regions. The simple answer is the so-called link atom (LA) approach,[7−9,14−18] in which the dangling bond in the QM region is usually capped by the hydrogen atom. Though the free valence of the dangling bond is covered by the H-link atom, this H-link atom leads to neglect of the electronic effect of the real substituent which is eliminated from the QM region and treated in the MM region.[19−21] As a result, this simple H-link atom method gives rise to considerable error in the study of transition metal complexes because the electronic structure of the metal center is sensitive to the ligands, as will be discussed in this paper.

Another approach to solve the boundary problem is the localized self-consistent field (LSCF) method by Rivail et al.[22] In the LSCF method, the frozen localized orbital is employed to fix the free valence. Since this method does not introduce the extra atom in the QM region, the electronic structure near the boundary is kept as it is in the real system. However, it is difficult to change the direction of the frozen orbital which should be orthogonalized to the other orbitals in the QM region, when the geometry changes occur in reaction or dynamics, for example.[22d] Gao et al. proposed another strategy called the

* Author to whom correspondence should be addressed. E-mail: sakaki@moleng.kyoto-u.ac.jp.
[†] Department of Molecular Engineering, Graduate School of Engineering.
[‡] Fukui Institute for Fundamental Chemistry.

10.1021/jp710310s CCC: $40.75
Published on Web 02/13/2008

SCHEME 1

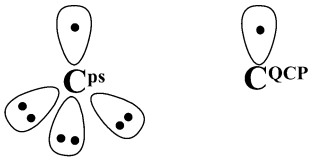

(a) Pseudobond approach **(b) QCP**

generalized hybrid orbital (GHO) method to solve the orthogonalization problem.[23] In the GHO method, four orbitals are placed on the boundary atom to represent sp^3 hybrids; one of them is the active orbital, which is included in the QM calculation, and the other three orbitals are treated as auxiliary frozen orbitals, which are necessary to satisfy the orthogonal condition. The GHO method is now employed in many studies of dynamics of proteins.[24]

The alternative approach to large molecules is the ONIOM method developed by Morokuma and his co-workers.[13,25] In the ONIOM method, a whole system is separated into an important region (model) and the other region; for example, in the 2-layer ONIOM (ONIOM2) method, the energy of the total system is represented by the sum of the high level (expensive) calculation of the model and the difference between low level (inexpensive) calculations of the model and real systems, as shown below:

$$E_{\mathrm{ONIOM2}} = E_{\mathrm{low,real}} - E_{\mathrm{low,model}} + E_{\mathrm{high,model}} \qquad (1)$$

where the terms "low" and "high" in subscript mean the computational level to be applied. In the model system, extra atoms must be introduced to cap dangling bonds, when the real system is one molecule. Thus, the ONIOM method has the same problem of electronic structure deviation as the LA approach.

Several approaches have been tried to solve this boundary problem in the LA approach. Antes and Thiel used the specially parametrized link atom called the adjusted connection atom.[16] This method improves the electronic structures near the boundary, but it has been implemented only for the semiempirical method. For the *ab initio* and DFT methods, Zhang et al. proposed a pseudobond approach,[26] in which the boundary atom has seven electrons, like halogen atom, as shown in Scheme 1, and the electronic property of the real system (usually sp^3 carbon atom) is reproduced with the effective core potential (ECP). This strategy is simple but reproduces well the charge and geometrical features. DiLabio et al. proposed a similar scheme called the quantum capping potential (QCP) method[27] for the *ab initio* and DFT methods. In the QCP method, the electronic properties are also reproduced with the parametrized ECP, but the boundary atom has only one electron, like hydrogen atom. The conventional ECP format is employed in these methods, and thus these methods can be easily applied to various systems. Yasuda and Yamaki reported a similar method, which is called minimum principle.[28] In this method, the effective potential was placed not only on the boundary atom but also on the atom attached to the boundary atom. Recently, Slaviček and Martínez proposed a multicentered valence electron effective potential (MC-VEEP) method[29] based on QCP. They introduced the effective potentials to the hydrogen atom of the methyl group to reproduce the exchange repulsion, while the hydrogen atom has no basis set. Poteau and co-workers recently developed an effective group potential (EGP) method[30] to replace functional groups such as SiH_3, PH_3, NH_3, CO, or Cp (cyclopentadienyl) by an imaginary system bearing bonding electrons and effective potential without nucleus. In the EGP method, the effective potential includes a generalized projection operator unlike the pseudobond approach and the QCP method. This leads to the generality of the theory. They succeeded in calculating large transition metal complexes with *ab initio* methods such as the CASPT2 method[30c] by reducing the number of electrons explicitly treated. However, it is not easy to use this method in practice because the EGP method does not use the conventional ECP format.

In many transition metal complexes, the tertiary phosphine (PR_3) is used as ligand. Because the large tertiary phosphine considerably increases the size of the transition metal complex, the CASPT2 and CCSD(T) methods cannot be applied to the transition metal complexes with such large phosphine. Thus, it is worth representing the large alkyl group of tertiary phosphine with the QCP method. The lone pair orbital of tertiary phosphine plays important roles in the coordinate bond of tertiary phosphine. This means that the parameters of the QCP should be determined so as to reproduce the lone pair orbital energy of PR_3. The same idea was previously proposed by Koga and Morokuma with a different shift operator.[31] In their method, the Coulomb integral of a chosen orbital of a model system is shifted to reproduce the lone pair orbital energy of the real system.

In this paper, first, we wish to report how to construct the QCP method to reproduce the lone pair orbital energy of PR_3, where R is an alkyl group such as Me (methyl), Et (ethyl), ^{i}Pr (isopropyl), and ^{t}Bu (*tert*-butyl). Because the lone pair orbital of PR_3 is HOMO and plays important roles as frontier orbital, such a parametrized QCP method is called frontier orbital consistent QCP (FOC-QCP), hereafter. Then, we will examine the performance of this method in the reductive elimination reaction of ethane from $M(Me)_2(PR_3)_2$ [M = Ni, Pd, Pt; R = Me, Et], which is one of the typical organometallic reactions. The next is to propose a new procedure to incorporate the steric effects of the real group into the model system with the post-HF method. This procedure is very effective; note that the steric repulsion has not been corrected well in the most QM/MM methods but the correction of steric repulsion is necessary to present a reliable result, as will be shown in this work. Also, we will evaluate the coordination energies of small molecules (CO, H_2, N_2, and C_2H_4) with $[RhCl(P^iPr_3)_2]_2$, using the combination of the CCSD(T), FOC-QCP, and SRC methods, to compare the theoretically evaluated binding energies with the experimental values.[32]

2. Theory. The FOC-QCP Method and Parametrization

First, we wish to mention the outline of the QCP method and how to determine the effective potentials for the tertiary phosphine. As described above, the QCP method employs the conventional ECP format:

$$U^{\mathrm{EP}} = U_L(r) + \sum_{l=0}^{L-1} \sum_{m=-l}^{l} \{U_l(r) - U_L(r)\}|l,m\rangle\langle l,m| \qquad (2)$$

where the U_l is the effective potential which comes from the individual Fock equation (eq 3) and the L is the maximum quantum number of angular momentum of projection operator.

$$(-1/2\nabla^2 - Z_v/r + U_l + W_l)\chi_l = \epsilon_l\chi_l \qquad (3)$$

The χ_l is the shape-consistent pseudo-orbital constructed by all-electron atomic valence orbitals, and the ϵ_l is the corresponding orbital energy. The Z_v is the effective nuclear charge, which is usually taken to be equal to the number of valence electrons. The W_l includes Coulomb and exchange integrals between the

valence electrons. The U_l effectively replaces the core-valence Coulomb and core-valence exchange terms of the all-electron operator. In the conventional codes, the individual U_l is represented by Gaussian expansion, eq 4:

$$U_l(r) = r^{-2} \sum_i C_{li} r^{n_{li}} \exp(-\zeta_{li} r^2) \tag{4}$$

where n_{li} is an integer of 0, 1, or 2.

The first step is to set the conventional ECP and the valence basis set of carbon atom. Usually, the ECP of carbon atom is used to replace two 1s electrons, while four electrons of 2s and 2p orbitals are explicitly treated as valence electrons. In this case, the effective nuclear charge Z_v is four. In the QCP method, on the other hand, three valence electrons are further replaced by ECP, and therefore, the effective nuclear charge becomes one ($Z_v = 1$). Consistent with this nuclear charge, the Coulomb term in the Fock operator must be decreased from $-4/r$ to $-1/r$. To consider this Coulomb term, the $-3/r$ term is added to the usual ECP for carbon. The ECP should decay as the distance becomes larger, because of the screening by the electrons in valence shell. Thus, the additional exponential term ($\exp(-\zeta r^2)$) is added to decrease the ECP as the distance increases. As a result, eq 5 is employed here, in which the power $(n - 2)$ of r is taken to be -1,

$$U_l(r)_{\mathrm{QCP}} = U_l(r) + C r^{n-2} \exp(-\zeta r^2) \tag{5}$$

where $U_l(r)$ means conventional ECP for carbon.

In the original QCP method, the exponent ζ value is fixed to be 1.29 and the coefficient is optimized so as to reproduce the geometrical features and Mulliken populations of ethane in which one of methyl groups is replaced with the QCP carbon atom (C^{QCP}). In the MC-VEEP method, on the other hand, the sum of coefficients is fixed to be -3.

In eq 5, we need to optimize the coefficient C and the exponent ζ of the additional term. Preliminarily, we investigated the dependency of the computational results on the coefficient, in which the FOC-QCP method was applied to the reductive elimination of ethane from Pt(II) complex. The coefficient was arbitrarily assumed to be -2.8, -2.9, -3.0, -3.1, and -3.2. Then, the ζ value was numerically optimized for each coefficient value, so as to reproduce frontier orbital energy, where the space distribution of the frontier orbital was not considered. The activation barrier and the reaction energy little depend on the coefficient value; see Supporting Information Table S1. From these results, we decided to employ -3 for the coefficient C and numerically optimized the ζ value for this coefficient value.

Now, let us start to discuss the FOC-QCP for PR_3. The model system is represented as $PC^{\#(R)}{}_3$, where $C^{\#(R)}$ means the pseudo-carbon atom parametrized for the R group; for example, $C^{\#(Me)}$ is a model of the Me group. The lone pair orbital of PR_3, which is HOMO, is frontier orbital because PR_3 coordinates to the metal with its lone pair orbital. This lone pair orbital interacts with the d orbital of the metal to significantly influence the energy level and the expansion of the d orbital of the metal, as shown in Scheme 2. The d orbital further interacts with the substrates and/or the other ligand which are at the position *trans* to PR_3. It is likely that the electronic effects of PR_3 can be reproduced well if the lone pair orbital energy of PR_3 is reproduced by the FOC-QCP method. Thus, we numerically optimized the exponent ζ value, as described above.

The combination of basis set and ECP are also important. In the QCP and MC-VEEP methods, the even-tempered (5s5p1d)/[5s5p1d] basis set[33] was employed. This basis set is, however,

SCHEME 2

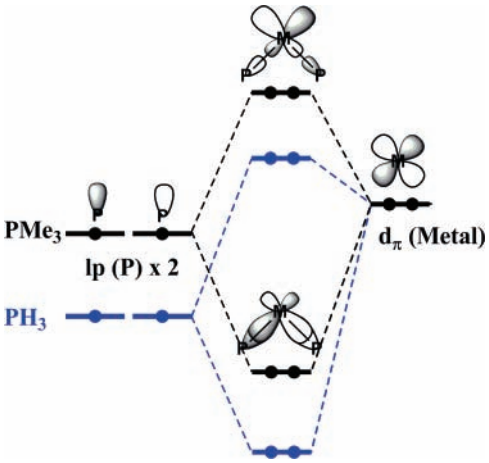

expensive. Here, the (4s4p)/[1s1p] basis set was employed for carbon atom with the corresponding ECP by Christiansen et al.,[34] which are the usual valence basis set and ECP named as CRENBL,[34] because the basis set size is reasonable. The combination of this basis set and the FOC-QCP reproduces well the lone pair orbital energy of PR_3, as will be discussed below.

Also, there are several candidates for computational methods to be employed to optimize the parameters. In the QCP and the MC-VEEP methods, the HF method was employed. In the pseudobond approach, the hybrid density functional method (B3LYP) was employed. Here, we employed both of the computational methods, the HF and the hybrid density functional method (B3PW91),[35] for parametrization, and examined which is better.

3. Computational Details

The geometry of PR_3 was optimized by the DFT[B3PW91] method with 6-31G basis sets,[36,37] where a d-polarization function was added to P. In each geometry, the vibration frequencies were calculated to confirm that it was an equilibrium structure. The orbital energies were calculated with the HF and the DFT[B3PW91] methods, where the cc-pVDZ basis sets were employed for all atoms.[38]

Geometries of transition metal complexes were optimized with the DFT[B3PW91] method, where core electrons of Ni (up to 2p), Pd and Rh (up to 3d), and Pt (up to 4f) were replaced with the effective core potentials (ECPs) of the Stuttgart−Dresden−Bonn (SDB) group[39,40] and their valence electrons were represented by (311111/22111/411/1) basis set[39] for Ni and (311111/22111/411) basis sets[40] for Pd, Pt, and Rh. For the PR_3, 6-31G basis sets[36,37] were employed, where a d-polarization function was added to P. For the other atoms, 6-31G(d,p)[36] basis sets were employed, where one diffuse function was added to Cl.[41] This basis set system is called hereafter BS-1. Vibrational frequencies were calculated with the DFT[B3PW91]/BS-1 method in all the stationary points to check if they were either equilibrium structure or transition state. The energies were evaluated with the CCSD(T), MP4(SDQ), and DFT[B3PW91] methods by using the DFT[B3PW91]-optimized geometries. In the energy evaluation, the better basis set system (BS-2) was employed as follows. For Pd, Pt, and Rh, two f polarization functions[42] were added to the above-described basis sets with the same ECPs. For Ni, the cc-pVTZ basis set[43] was employed because the cc-pVTZ basis set or a better one should be used for Ni to present reliable energy change with the CCSD(T) method,[4] while a g polarization

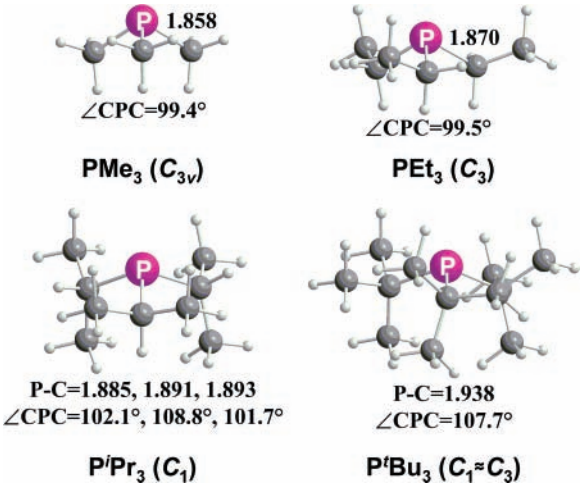

Figure 1. Geometries of PMe_3, PEt_3, P^iPr_3, and P^tBu_3 optimized with the DFT[B3PW91]/BS-1 method. Bond lengths are in angstroms, and bond angles are in degrees. In parentheses are point groups.

TABLE 1: The HOMO Energies (eV) Calculated with the DFT(B3PW91) and RHF Methods of PH_3, PMe_3, PEt_3, P^iPr_3, and P^tBu_3

	PH_3	PMe_3	PEt_3	P^iPr_3	P^tBu_3
B3PW91	−7.56	−6.06	−5.98	−5.74	−5.55
RHF	−10.53	−8.90	−8.78	−8.49	−8.22

TABLE 2: The Parameters of Additional Effective Potential for $C^{\#(R)}$ Optimized with RHF and DFT[B3PW91] Methods

			z	
PR_3	n	C	RHF	B3PW91
PMe_3	1	−3.0	1.46997334	1.58297547
PEt_3	1	−3.0	1.49525346	1.60203115
P^iPr_3	1	−3.0	1.48708431	1.59434019
P^tBu_3	1	−3.0	1.49195717	1.59406618

function was removed. For H_2 molecule and chlorine atom, aug-cc-pVDZ basis sets were used, while for the other atoms, cc-pVDZ basis sets were employed. Solvent effects were also considered with the PCM method using the integral equation formalism,[44] where the temperature was taken to be 303.15 K.

All the calculations were performed with the Gaussian03 program package.[45] To optimize the parameter of the FOC-QCP, the STEPIT ver. 7.7 program[46] was employed in combination with Gaussian03.

4. Results and Discussion

4.1. Frontier Orbital Consistent Quantum Capping Potential (FOC-QCP) for PR_3. Geometries and important geometrical parameters of PH_3, PMe_3, PEt_3, P^iPr_3, and P^tBu_3 are shown in Figure 1. Their HOMO (lone pair orbital) energies were calculated with the RHF and DFT[B3PW91] methods, as shown in Table 1. The HOMO energy of PH_3 is considerably lower than that of PMe_3 by about 1.5 eV, and the HOMO energy becomes higher upon going from PMe_3 to P^tBu_3. This means that, in a bulky phosphine such as P^tBu_3, we should carefully consider not only the steric effect but also the electronic effect.

Table 2 lists the parameters of the additional effective potentials for each PR_3 group optimized by the RHF and DFT-[B3PW91] methods. In the parametrization of $C^{\#(iPr)}$, three carbon atoms bound with phosphorus atom were treated equivalently, whereas they are not equivalent, strictly speaking (see Figure 1). This procedure is reasonable because the difference among these three carbon atoms is small and the rotation of phosphine would occur around the M−P bond. The RHF-optimized ζ values are somewhat smaller than the DFT-[B3PW91]-optimized ones. The reason is not clear. It is noted that no clear relation between the ζ value and the lone pair orbital energy is observed; for example, the lone pair orbital energy of PMe_3 is lower than that of PEt_3, and the ζ value of $C^{\#(Me)}$ is smaller than that of $C^{\#(Et)}$. On the other hand, the lone pair orbital energy of PEt_3 is lower than that of P^iPr_3 but the ζ value of $C^{\#(Et)}$ is slightly larger than that of $C^{\#(iPr)}$. These results suggest that neither extrapolation nor interpolation can be applied to optimization of the ζ value; in other words, the ζ value must be optimized independently for each PR_3.

4.2. Application of the FOC-QCP Method to the Reductive Elimination Reaction of Ethane from $M(Me)_2(PR_3)_2$ [M = Ni, Pd, or Pt; R = H or Me]. This reaction was investigated with the CCSD(T), MP4(SDQ), and DFT[B3PW91] methods, where DFT[B3PW91]-optimized geometries were employed; see Figure 2 and Figure S1 for the geometry changes by the reductive elimination from $M(Me)_2(PMe_3)_2$ and $M(Me)_2(PH_3)_2$, respectively.

A. Reliability of Computational Methods. Before starting to examine the performance of the FOC-QCP method, we wish to investigate the reliability of computational methods such as the RHF, MP2 to MP4(SDQ), CCSD, CCSD(T), and DFT-[B3PW91] methods. Here, we employed PH_3 to reduce the size of the complex. For the nickel complex, the MP2 to MP4(SDQ) methods present unreasonable results, as shown in Table 3. The reason was previously discussed in terms of very large electron correlation effects in the nickel complex.[3,4] Although the electron correlation effects are expected to be small in a 4d metal such as palladium, the MP4(SDQ) method presents considerably different results from those of the CCSD(T) method. Moreover, the activation barrier is considerably different among the MP4-(D), MP4(DQ), and MP4(SDQ) methods. This significantly large difference suggests that the MP4(SDQ) method does not present reliable energy changes in the reductive elimination of the palladium complex. In the platinum complex, on the other hand, the MP4(SDQ) method presents similar results to the CCSD(T) method and the activation barrier is little different among the MP4(D), MP4(DQ), and MP4(SDQ) methods. It is also noted that the large activation barriers calculated with these methods are consistent with the experimental result that the reductive elimination reaction does not occur in the platinum complex.[47] The reason was clearly discussed by Low and Goddard.[48] From these results it should be concluded that the MP4(SDQ) method presents reasonable results in the reductive elimination of the platinum complex but does not in the palladium and nickel complexes.

The DFT[B3PW91] method presents somewhat smaller activation barriers and somewhat larger exothermicities than does the CCSD(T) method in all cases. Although it is not clear which of the CCSD(T) and DFT[B3PW91] methods is more reliable, at this moment, we will discuss in section 4.4 that the CCSD(T)-calculated results are much better than the DFT-[B3PW91]-calculated ones.

Among these computational methods, the CCSD(T) method is the most reliable. The computational cost of the CCSD(T) method is, however, too large to be applied to the real system with R = Me. The best way to present reliable results for the reductive elimination is to employ the CCSD(T) method with the FOC-QCP method, as will be discussed below.

B. Energy Changes Calculated with the FOC-QCP Method. Here, we wish to discuss the performance of the FOC-QCP method. The activation barriers and reaction energies calculated

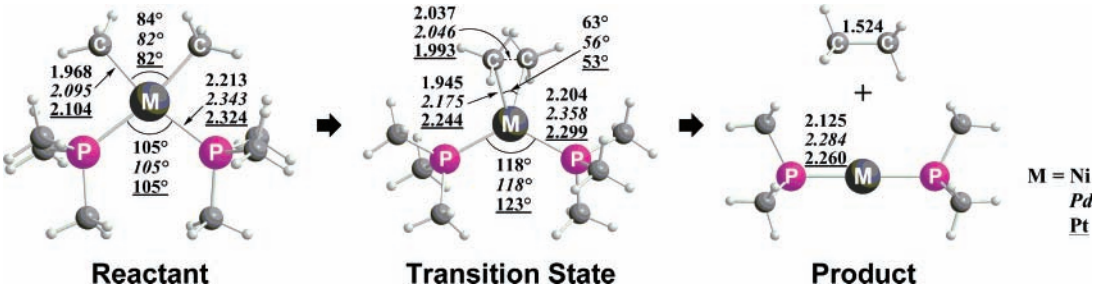

Figure 2. Geometry changes by the reductive elimination of ethane from $M(Me)_2(PMe_3)_2$ (M = Ni, Pd, Pt) optimized with the DFT[B3PW91]/BS-1 method. Bond lengths are in angstroms, and bond angles are in degrees. Upper: M = Ni. Middle: M = Pd. Bottom: M = Pt.

TABLE 3: The Activation Barriers (E_a) and the Reaction Energies (ΔE) of the Reductive Elimination Reaction of C_2H_6 from $M(Me)_2(PH_3)_2$

	Ni		Pd		Pt	
method	E_a	ΔE	E_a	ΔE	E_a	ΔE
RHF	61.7	−0.8	34.1	−48.5	61.7	−23.3
MP2	−64.1	−82.3	21.9	−17.6	44.4	−0.8
MP3	67.5	28.1	33.4	−23.9	56.0	−7.7
MP4(D)	−55.9	−77.6	26.1	−22.5	50.0	−5.0
MP4(DQ)	−72.0	−97.5	24.7	−25.6	50.5	−6.0
MP4(SDQ)	−86.2	−110.8	18.7	−27.0	49.5	−4.9
CCSD	27.2	−2.9	30.9	−22.1	54.4	−5.2
CCSD(T)	18.7	−6.5	29.5	−18.0	52.0	−2.0
DFT[B3PW91]	17.7	−13.8	26.0	−26.8	48.1	−9.0

TABLE 4: The Activation Barriers (E_a) and the Reaction Energies (ΔE) (kcal/mol) of the Reductive Elimination Reaction of C_2H_6 from $M(Me)_2(PR_3)_2$

	B3PW91		MP4(SDQ)		CCSD(T)	
R	E_a	ΔE	E_a	ΔE	E_a	ΔE
		M = Ni				
Me	20.4	−14.0	−83.6	−109.9	N/A	N/A
H	17.7	−13.8	−86.2	−110.8	18.7	−6.5
$C^{\#(Me)}$ ζ(RHF)	–	–	−94.5	−125.9	20.3	−4.9
$C^{\#(Me)}$ ζ(B3PW91)	20.2	−13.5	−83.5	−114.7	21.8	−5.2
		M = Pd				
Me	30.7	−26.4	22.8	−24.9	N/A	N/A
H	26.0	−26.8	18.7	−27.0	29.5	−18.0
$C^{\#(Me)}$ ζ(RHF)	–	–	18.7	−25.9	31.8	−14.8
$C^{\#(Me)}$ ζ(B3PW91)	29.3	−24.9	19.8	−26.4	32.8	−15.1
		M = Pt				
Me	51.6	−11.7	53.3	−5.0	N/A	N/A
H	48.1	−9.0	49.6	−4.9	52.0	−2.0
$C^{\#(Me)}$ ζ(RHF)	–	–	50.8	−4.7	54.5	−0.3
$C^{\#(Me)}$ ζ(B3PW91)	51.9	−9.6	52.2	−5.6	56.0	−1.2
$C^{\#(Me)}$ + SRC ζ(RHF)	–	–	52.1	−5.7	54.5	−1.1
$C^{\#(Me)}$ + SRC ζ(B3PW91)	51.2	−11.9	52.2	−6.5	56.0	−2.0

with the FOC-QCP method are listed in Table 4, where the R = $C^{\#(Me)}$ represents that the methyl groups of PMe_3 are substituted for $C^{\#(Me)}$, and the ζ(RHF) and ζ(B3PW91) represent the ζ values determined by RHF and DFT[B3PW91] methods, respectively. As shown in Table 4, the DFT[B3PW91]-calculated activation barrier of the R = $C^{\#(Me)}$ system agrees well with the activation barrier of the real system, where the error is 0.2, 1.4, and 0.3 kcal/mol for Ni, Pd, and Pt complexes, respectively. These results indicate that the FOC-QCP can reproduce well the electronic effect of PMe_3 in the DFT-[B3PW91] calculation. In the PH_3 model system, on the other hand, the DFT[B3PW91] method presents somewhat smaller activation barriers than those for the real systems; the error is 2.7, 4.7, and 3.5 kcal/mol for Ni, Pd, and Pt complexes, respectively. These errors are not different very much between PH_3 and $PC^{\#(Me)}_3$ systems but not negligibly small. The DFT-[B3PW91]-calculated exothermicities of the R = $C^{\#(Me)}$ system are also moderately smaller than those of the real system. This

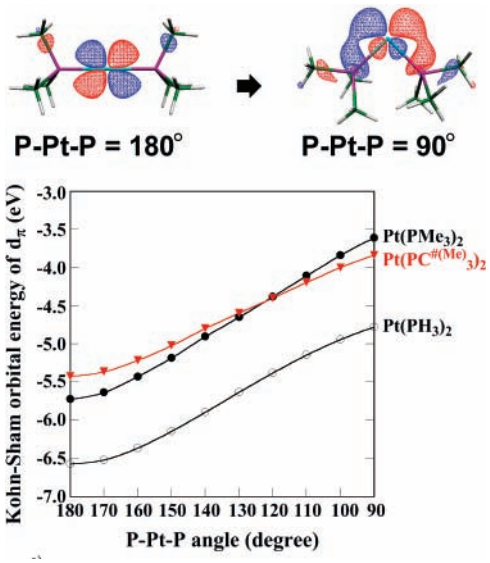

Figure 3. The molecular orbital (Kohn−Sham orbital) energies of HOMO of $Pt(PR_3)_2$ (R = Me, H, and $C^{\#(Me)}$) vs the P−Pt−P angle. The DFT[B3PW91]/BS-2 method.

discrepancy becomes considerably small by making a steric repulsion correction, which will be discussed below.

The MP4(SDQ)-calculated energy changes of the R = $C^{\#(Me)}$ system are compared with those of the real system in the platinum complex, because the MP4(SDQ) method presents reliable energy change in the reductive elimination of the platinum complex but not at all in the reductive elimination of the nickel complex. The MP4(SDQ)-calculated activation barrier and reaction energy of the R = $C^{\#(Me)}$ system agree well with those of the real system (R = Me), when the ζ(B3PW91) value is employed. On the other hand, the use of the ζ(RHF) value leads to moderate underestimation of the activation barrier. Similar results are observed in the Pd complexes with $C^{\#(Me)}$. From these results, it is concluded that the ζ(B3PW91) value should be used in the post HF calculation.

The activation barriers calculated with the CCSD(T) method are always larger than those of the DFT[B3PW91] and MP4-(SDQ) methods; for example, in the platinum complex with PH_3, the activation barrier is calculated to be 48.1, 49.6, and 52.0 kcal/mol by the DFT[B3PW91], MP4(SDQ), and CCSD(T) methods, respectively. The system with R = $C^{\#(Me)}$ reproduces well this trend. Similar results are observed in the nickel and palladium complexes with PH_3; for instance, the activation barrier is calculated to be 17.7 and 26.0 kcal/mol for the nickel and palladium complexes, respectively, with the DFT[B3PW91] method and 18.7 and 29.5 kcal/mol, respectively, with the CCSD(T) method. The DFT[B3PW91]-calculated exothermicities are always larger than the CCSD(T)-calculated values in both PH_3 and $PC^{\#(Me)}_3$ systems. For instance, the DFT[B3PW91]

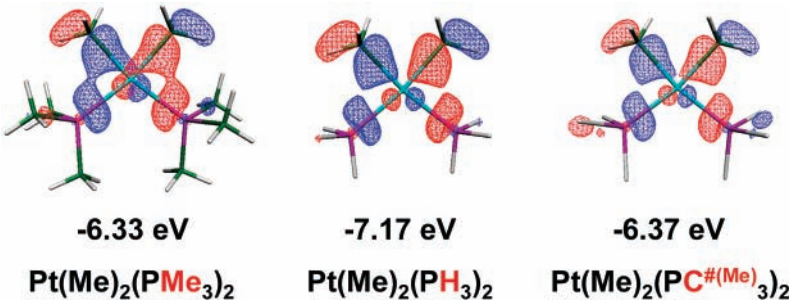

Figure 4. Bonding orbitals and orbital energy (Kohn−Sham orbital) of $Pt(Me)_2(PR_3)_2$. Surface value is 0.05 au. The DFT[B3PW91]/BS-2 method.

SCHEME 3

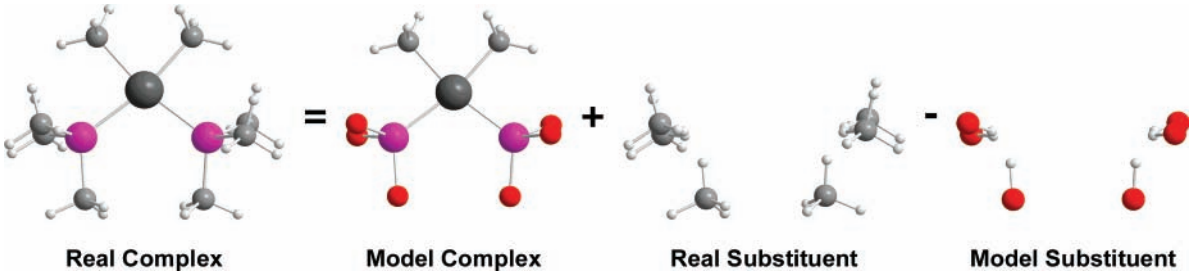

method overestimates the exothermicity by 7 to 9 kcal/mol for the PH_3 complex and by 8 to 10 kcal/mol for the $PC^{\#(Me)}{}_3$ complexes, compared to those of the CCSD(T) method. The MP4(SDQ) method similarly overestimates the exothermicity, compared to the CCSD(T) method in both PH_3 and $PC^{\#(Me)}{}_3$ complexes. From these results, it is concluded that the FOC-QCP method can reproduce well the energy changes of the real system and that the CCSD(T) method with the FOC-QCP presents better results of this type of reductive elimination reaction than the DFT[B3PW91] and MP4(SDQ) methods.

C. Electronic Effect of $PC^{\#(Me)}{}_3$. We also examined if the electronic effect is reproduced well by the FOC-QCP method. Figure 3 shows the frontier orbital energy of $Pt(PR_3)_2$ (R = Me, H, or $C^{\#(Me)}$) as a function of the P−Pt−P angle from 180° to 90°, where the Kohn−Sham orbital energy is given. The frontier orbital energy of $Pt(PH_3)_2$ is considerably different from that of $Pt(PMe_3)_2$ due to the difference in the lone pair orbital energy between PH_3 and PMe_3. However, the orbital energy of $Pt(PC^{\#(Me)}{}_3)_2$ as well as its dependence on the P−Pt−P angle agrees well with those of $Pt(PMe_3)_2$. In $Pt(Me)_2(PR_3)_2$ (R = Me, H, or $C^{\#(Me)}$), the FOC-QCP method also reproduces well the energy of the Pt−Me bonding orbital, as shown in Figure 4, while the orbital energy of the simple model $Pt(Me)_2(PH_3)_2$ is considerably different from that of the real complex. Because this Pt−Me bonding orbital mainly participates in the reductive elimination, it is necessary to reproduce correctly the energy level and the shape of this molecular orbital. This is the reason why the activation barrier of the simple model is different from that of the real system but the FOC-QCP method can reproduce well the activation barrier and the reaction energy of the real system.

4.3. Energy Change of Reductive Elimination of Ethane from $Pt(R^1)_2(PR^2{}_3)_2$ [R^1 = Me, R^2 = Et, ^{i}Pr, and R^1 = H, R^2 = ^{t}Bu] with Steric Repulsion Correction (SRC). The steric effects of two PMe_3 groups are not included in the above calculation with the FOC-QCP, because the steric effect is not large in PMe_3. However, the steric repulsion must be taken into consideration for bulky *tert*-phosphine. We wish to propose here a new procedure for the steric repulsion correction (SRC), as shown in Scheme 3. In this procedure, total energy is represented by eq 6,

$$E = E_{MC} + E_{RS} - E_{MS} \quad (6)$$

where the subscripts MC, RS, and MS represent model complex, real substituent, and model substituent, respectively. The difference of the latter two terms of Scheme 3 and eq 6 corresponds to the steric repulsion correction. This evaluation is similar to but not the same as the ONIOM method, because the latter two terms of Scheme 3 and eq 6 do not include the active region in this procedure. This is also similar to the G2 method[49] to some extent; remember that the G2 method incorporates the basis set effects as the difference between MP2 calculation with basis sets of high quality and those with basis sets of low quality.

In the platinum complex $Pt(Me)_2(PMe_3)_2$, the SRC is calculated with the various computational methods (Table 5). All the SRCs are negligibly small except for the reaction energy (ΔE) calculated with the RHF and the DFT[B3PW91] methods. It is noted that the reaction energy calculated with the DFT-[B3PW91] method is considerably improved with this SRC; for instance, the error of the DFT[B3PW91]-calculated reaction energy is 2.1 kcal/mol without the SRC but decreases to 0.3 kcal/mol after the SRC, as shown in Table 4, which agrees well with the reaction energy of the real system. Interestingly, the

TABLE 5: The Steric Repulsion Correction of the Activation Barrier (E_a) and the Reaction Energy (ΔE) (kcal/mol) in the Reductive Elimination Reaction of C_2H_6 from $Pt(Me)_2(PMe_3)_2$

	$C^{\#(Me)}$ ζ (RHF)		$C^{\#(Me)}$ ζ (B3PW91)	
method	E_a	ΔE	E_a	ΔE
B3PW91	−	−	−0.7	−2.3
RHF	−0.6	−2.2	−0.5	−2.0
MP2	0.1	−0.7	0.1	−0.6
MP3	0.0	−0.9	0.0	−0.8
MP4(D)	0.0	−1.0	0.0	−0.9
MP4(DQ)	−0.1	−1.1	0.0	−0.9
MP4(SDQ)	−0.1	−1.0	0.0	−0.9
CCSD	−0.1	−1.1	0.0	−0.9
CCSD(T)	0.0	−0.9	0.0	−0.8

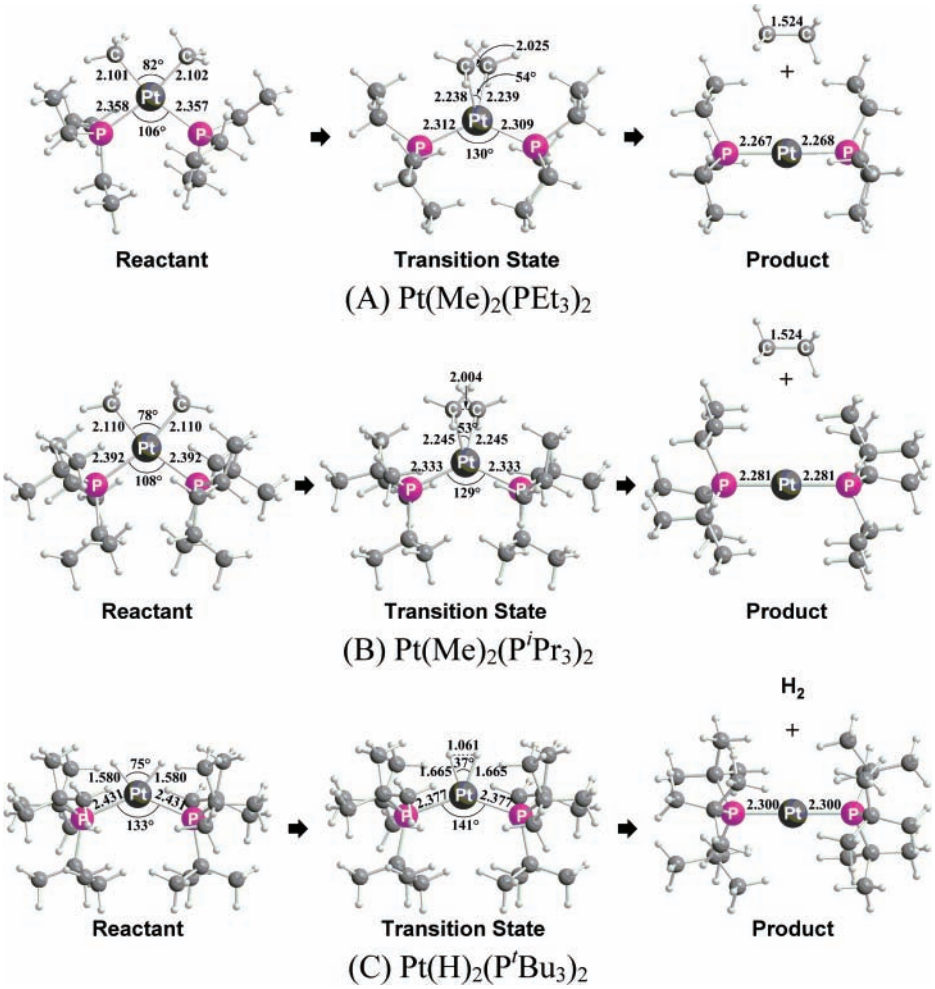

Figure 5. DFT[B3PW91]/BS-1-optimized geometry changes by the reductive elimination reaction of C_2H_6 from $Pt(Me)_2(PEt_3)_2$ and $Pt(Me)_2(P^iPr_3)_2$ and that of H_2 from $Pt(Me)_2(P^tBu_3)_2$. Bond lengths are in angstroms, and bond angles are in degrees.

SRC is almost the same in the MP2 to MP4(SDQ), CCSD, and CCSD(T) methods because the systems calculated in the SRC do not include the transition metal element. This means that the MP2 method is useful enough to evaluate the SRC.

The reason why the SRCs are large in the RHF and DFT-[B3PW91] calculations is easily understood in terms of the weak point of these methods; these methods cannot incorporate well dispersion interaction, indicating that the steric repulsion is overestimated. The ζ(B3PW91) value provides better activation barrier and reaction energy than does the ζ(RHF) value after the steric repulsion correction, too.

In more bulky ligands such as PEt_3, P^iPr_3, or P^tBu_3, the SRC becomes crucially important, as expected. We calculated the activation barrier and reaction energy of the reductive elimination of C_2H_6 from $Pt(Me)_2(PEt_3)_2$ and $Pt(Me)_2(P^iPr_3)_2$ and the reductive elimination of H_2 from $Pt(H)_2(P^tBu_3)_2$ (see Figure 5) with the DFT[B3PW91], MP4(SDQ), and CCSD(T) methods. As shown in Table 6, when the SRC is not included, the activation barrier and the reaction energy of the model $C^{\#(Et)}$ are considerably larger than those of the real complex by 4.8 and 7.8 kcal/mol, respectively, in the DFT[B3PW91] calculations. However, the activation barrier and the reaction energy with the SRC (see the column of $C^{\#(Et)}$ + SRC) agree well with those of the real system, where the SRC was evaluated with the DFT[B3PW91] method. Also, the MP4(SDQ)-calculated activation barriers and reaction energies with SRC agree well with those of the real system (Table 6) in the PEt_3 complex, where the SRCs are evaluated with the MP2 method. Also in the P^iPr_3 and P^tBu_3 complexes, the SRC significantly improves the activation barriers and reaction energies in the DFT[B3PW91] calculation. For the P^tBu_3 complex, Morokuma and his co-workers previously reported the energy change of the oxidative addition of H_2 to $Pt(P^tBu_3)_2$, which is the reverse reaction of reductive elimination investigated here, by using ONIOM2(MP2:MM3)[50] and ONIOM3-(CCSD(T):MP2:MM3) methods.[51] In those works, the activation barrier and the reaction energy were calculated to be 8.5 and −6.0 kcal/mol, respectively, by the ONIOM2-(MP2:MM3) method, and 10.1 and −4.1 kcal/mol, respectively, by the ONIOM3(CCSD(T):MP2:MM3) method. Interestingly,

TABLE 6: The Activation Barriers (E_a) and the Reaction Energies (ΔE) (kcal/mol) of the Reductive Elimination Reaction of C_2H_6 from $Pt(Me)_2(PEt_3)_2$ and $Pt(Me)_2(P^iPr_3)_2$ and H_2 from $Pt(Me)_2(P^tBu_3)_2$, Where the SRCs Are Calculated with the MP2 Method

	B3PW91		MP4(SDQ)		CCSD(T)	
R	E_a	ΔE	E_a	ΔE	E_a	ΔE
Et	43.1	−22.3	44.1	−12.9	N/A	N/A
$C^{\#(Et)}$	47.9	−14.5	47.9	−10.7	51.8	−5.9
$C^{\#(Et)}$ + SRC	43.6	−22.5	46.3	−13.6	50.2	−8.8
^{i}Pr	43.3	−25.0	N/A	N/A	N/A	N/A
$C^{\#(iPr)}$	48.3	−16.5	48.4	−12.9	52.5	−7.8
$C^{\#(iPr)}$ + SRC	45.2	−24.2	48.7	−14.8	52.9	−9.7
^{t}Bu	6.7	−6.3	N/A	N/A	N/A	N/A
$C^{\#(tBu)}$	9.6	−1.0	9.3	0.4	12.1	4.3
$C^{\#(tBu)}$ + SRC	7.2	−9.0	7.2	−6.2	10.0	−2.4

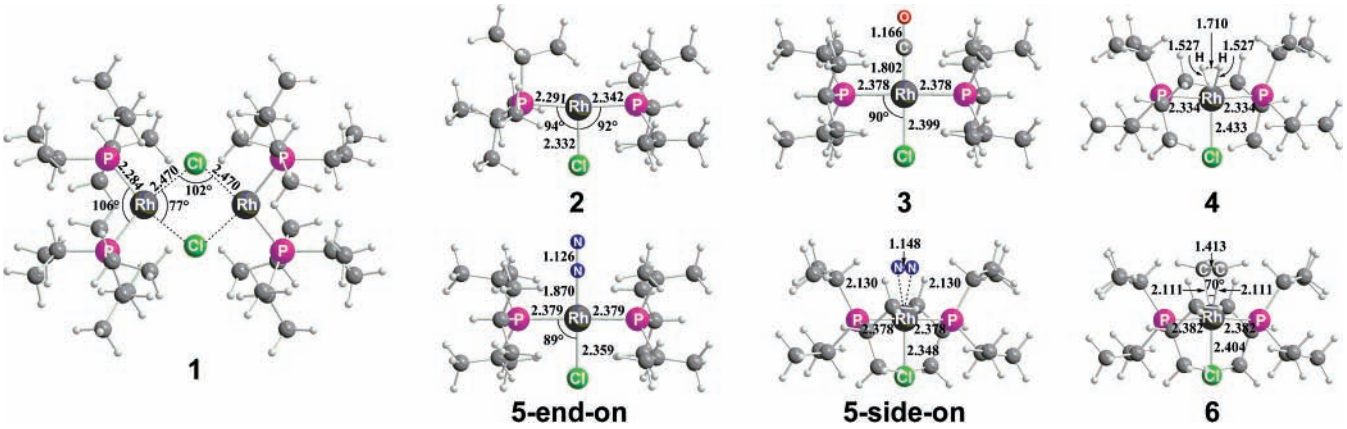

Figure 6. Geometries of $[RhCl(P^iPr_3)_2]_2$ **1**, $RhCl(P^iPr_3)_2$ **2**, $RhCl(P^iPr_3)_2(CO)$ **3**, $RhCl(P^iPr_3)_2(H)_2$ **4**, $RhCl(P^iPr_3)_2(N_2)$ **5-end-on** and **5-side-on**, and $RhCl(P^iPr_3)_2(C_2H_4)$ **6** optimized with the DFT[B3PW91]/BS-1 method. Bond lengths are in angstroms, and bond angles are in degrees.

TABLE 7: The Monomerization Energy of $[RhCl(P^iPr_3)_2]_2$ 1 and the Coordination Energies of CO, H_2, N_2, and C_2H_4 to 1 Calculated with the DFT[B3PW91] (in Vacuo), DFT[B3PW91] (in Toluene), DFT[B3PW91]/$C^{\#(i\mathrm{Pr})}$ + SRC, and CCSD(T)/$C^{\#(i\mathrm{Pr})}$ + SRC Methods (kcal/mol)

	B3PW91 real (in vacuo)	B3PW91 real (in benzene)	B3PW91 $C^{\#(i\mathrm{Pr})}$ + SRC (in vacuo)	CCSD(T) $C^{\#(i\mathrm{Pr})}$ + SRC (in vacuo)	exptl[a]
$[RhCl(P^iPr_3)_2]_2$ **1** → $2RhCl(P^iPr_3)_2$ **2**	12.5	12.7	13.6	33.0	> 17.8[c,d]
$(1/2)[RhCl(P^iPr_3)_2]_{2(soln)} + CO_{(g)} \rightarrow$ **3**$_{(soln)}$	−49.6	−47.9[b]	−52.1	−37.9	−39.3 ± 0.7[d]
$(1/2)[RhCl(P^iPr_3)_2]_{2(soln)} + H_{2(g)} \rightarrow$ **4**$_{(soln)}$	−23.4	−22.2[b]	−25.0	−20.3	−23.6 ± 0.6[d]
$(1/2)[RhCl(P^iPr_3)_2]_{2(soln)} + N_{2(soln)} \rightarrow$ **5-end-on**$_{(soln)}$	−18.4	−18.5	−23.6	−9.2	−7.6 ± 0.7[e]
$(1/2)[RhCl(P^iPr_3)_2]_{2(soln)} + N_{2(soln)} \rightarrow$ **5-side-on**$_{(soln)}$	−1.9	−2.8	−6.3	+6.1	
$(1/2)[RhCl(P^iPr_3)_2]_{2(soln)} + C_2H_{4(soln)} \rightarrow$ **6**$_{(soln)}$	−18.4	−21.0	−20.0	−18.7	−15.9 ± 0.6[e]

[a] ΔH values (kcal/mol) determined by calorimetrical method and/or by equilibrium method. [b] The energies of CO and H_2 molecule are calculated in vacuo. [c] This value is lower limit determined by spectroscopic observation (see ref 53). [d] Reference 53a. [e] Reference 53b.

the CCSD(T) method with the FOC-QCP + SRC presents almost the same activation barrier as and a similar reaction energy to those of the ONIOM3(CCSD(T):MP2:MM3) method.

At the end of this section, we wish to mention that the computational cost is considerably reduced by using this FOC-QCP method. The MP4(SDQ) calculation of the real complex (R = Et) needs about 30 h with 2 cpus of Itanium 2 (1.60 GHz), while that of the model complex (R = $C^{\#(Et)}$) needs less than 10 min with the same machine. To evaluate the SRC, we need to perform the MP2 calculations of six ethane molecules and six $C^{\#(Et)}$−H systems, which require 17 min and 2 s, respectively.[52]

By employing the FOC-QCP method with the SRC, the steric effects of the bulky substituent groups can be effectively considered at the MP2 level and the electronic effects of the real ligands can be incorporated well in the calculation at the CCSD(T) level.

4.4. CCSD(T)-Calculated Monomerization Energy of $[RhCl(P^iPr_3)_2]_2$ and Coordination Energies of CO, H_2, N_2, and C_2H_4 to $[RhCl(P^iPr_3)_2]_2$. It is worth making comparison between the theoretical energy change calculated by the FOC-QCP and the experimental value. The monomerization energy of $[RhCl(P^iPr_3)_2]_2$ **1** to $RhCl(P^iPr_3)_2$ **2** and the coordination energies of CO, H_2, N_2, and C_2H_4 with $[RhCl(P^iPr_3)_2]_2$ were experimentally reported previously.[32] We evaluated these energies by the DFT[B3PW91] and CCSD(T) methods with the FOC-QCP, where their geometries were optimized with the DFT method, as shown in Figure 6, and the SRC was calculated with the MP2 method (see Table 7). We wish to mention here that the solvation effect is very small in these reactions because the solvent is nonpolar benzene, indicating that the CCSD(T)-calculated value in vacuo can be compared with the experimental results.

The endothermicity of the monomerization was experimentally estimated to be larger than 17.8 kcal/mol in benzene at 303.15 K.[32a] The DFT[B3PW91] method, however, presents much smaller destabilization energy by the monomerization of **1** in both vacuo and benzene than the experimental lower limit. This DFT[B3PW91]-calculated result seems incorrect, as follows: The DFT[B3PW91] method overestimates the steric repulsion by bulky ligands between two monomers because the dispersion interaction cannot be taken into consideration well by the DFT[B3PW91] method. This means that the DFT[B3PW91] method underestimates the stability of dimer **1**, which leads to underestimation of the destabilization energy by the monomerization of **1**. On the other hand, the CCSD(T) method with the FOC-QCP and SRC presents much larger monomerization energy, which agrees well with the experimental value.

In $RhCl(P^iPr_3)_2(H_2)$ and $RhCl(P^iPr_3)_2(C_2H_4)$, the DFT[B3PW91]-calculated coordination energies agree well with the experimental results. However, it is likely that this agreement is a fortunate accident as follows: The dimer **1** was taken to be the standard of the coordination energy and the DFT[B3PW91] method underestimates the destabilization energy by the monomerization of **1**, as discussed above. These results indicate that the DFT[B3PW91] method underestimates the interaction energy of a small molecule such as H_2 and C_2H_4 with a monomer $RhCl(P^iPr_3)_2$. In other words, the DFT[B3PW91] method underestimates the destabilization energy by the monomerization of **1** and the stabilization energy by the coordination of a small molecule with $RhCl(P^iPr_3)_2$, which leads to the

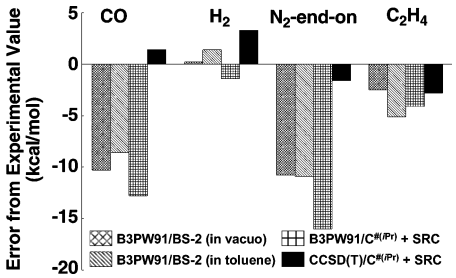

Figure 7. The error of the coordination energies (kcal/mol) of CO, H_2, N_2-end-on, and C_2H_4 to $[RhCl(P^iPr_3)_2]_2$ from the experimental values.

fortunate agreement of the DFT[B3PW91]-calculated binding energy with the experimental value.

In $RhCl(P^iPr_3)_2(N_2)$, two coordination modes, end-on and side-on, were experimentally reported by X-ray diffraction experiments,[53] while the theoretical investigation at the HF level indicated that the end-on coordination mode was more stable than the side-on mode.[54] Also, the DFT[B3PW91]-calculated coordination energies are −18.4 and −1.9 kcal/mol for end-on and side-on coordination modes, respectively, which clearly shows that the end-on coordination mode is much more stable than the side-on mode. However, both values do not agree with the experimental result (−7.6 ± 0.7 kcal/mol). On the other hand, the CCSD(T)-calculated coordination energy of the end-on mode agrees well with the experimental value.

It should be noted that the CCSD(T)-calculated coordination energies of CO, H_2, N_2, and C_2H_4 agree well with the experimental results within the error of about 3 kcal/mol, while the DFT[B3PW91]-calculated coordination energies considerably deviate from the experimental values, as shown in Figure 7. From these results, it is concluded that the CCSD(T) method should be applied to these complexes and that the FOC-QCP method with the SRC can present reliable coordination energies of such molecules as CO, H_2, N_2, and C_2H_4 with $[RhCl(P^iPr_3)_2]_2$.

5. Conclusions

Chemically reasonable models of PR_3 (R = Me, Et, ^{i}Pr, and ^{t}Bu) were constructed to perform the highly sophisticated post-Hartee−Fock calculations of the large transition metal complexes. The important role of PR_3 as a ligand is the σ-donation to the metal center with its lone pair orbital (HOMO). Because the strength of σ-donation, which relates to the strength of the *trans* effect, is determined by the lone pair orbital energy, we optimized the effective potential on the model atom ($C^{\#(R)}$) so as to reproduce the lone pair orbital energy of PR_3 (R = Me, Et, ^{i}Pr, ^{t}Bu) with the RHF and DFT[B3PW91] methods. We called this potential the frontier orbital consistent quantum capping potential (FOC-QCP).

First, we investigated the reductive elimination of ethane from model complexes $M(Me)_2(PH_3)_2$ (M = Ni, Pd, or Pt) with the DFT[B3PW91], MP2 to MP4(SDQ), CCSD, and CCSD(T) methods. Comparing to the CCSD(T) method, the DFT-[B3PW91] method tends to underestimate the activation barrier and overestimate the exothermicity of the reaction. The MP4-(SDQ) method cannot be applied to the reductive elimination reaction of the nickel and palladium complexes. In the reaction of the platinum complex, the MP4(SDQ) method slightly underestimates the activation barrier compared to the CCSD-(T) method. These results indicate that we must apply the CCSD(T) method to this reductive elimination. However, the CCSD(T) method cannot be applied to the real reaction systems, $M(Me)_2(PR_3)_2$, because of their large sizes. This is the reason why we need the FOC-QCP method.

To examine the performance of this FOC-QCP, we calculated the activation barriers and the reaction energies of the reductive elimination reactions of C_2H_6 and H_2 from $M(R^1)_2(PR^2_3)_2$ (M = Ni, Pd, or Pt; R^1 = Me for R^2 = Me, Et, or ^{i}Pr; R^1 = H for R^2 = ^{t}Bu) with the DFT[B3PW91], MP4(SDQ), and CCSD(T) methods.

In the reductive elimination reaction of ethane from $M(Me)_2$-$(PMe_3)_2$, the model ligand $PC^{\#(Me)}_3$ reproduces well the activation barriers and the reaction energies of the real reaction system in all the computational methods employed here except for the DFT[B3PW91]-calculated reaction energy of the $PC^{\#(Me)}_3$ system which somewhat deviates from that of the real system. However, the steric repulsion correction (SRC) leads to good agreement of this DFT[B3PW91]-calculated reaction energy with that of the $PC^{\#(Me)}_3$ and the real system.

In more bulky substituents such as Et, ^{i}Pr, and ^{t}Bu, the steric repulsion becomes crucially important to present correct energy changes. The correction of steric repulsion is carried out by calculating the substituent only, to which the MP2 method is successfully applied because the substituent systems do not include the transition metal element.

By using the FOC-QCP method combined with the SRC, the monomerization energy of $[RhCl(P^iPr_3)_2]_2$ and coordination energies of CO, H_2, N_2, and C_2H_4 with the $[RhCl(P^iPr_3)_2]_2$ were calculated with the DFT[B3PW91] and CCSD(T) methods. The CCSD(T)-calculated monomerization energy and coordination energies agree well with the experimental value; the rms error is 2.4 kcal/mol, which is much smaller than the rms error (7.6 kcal/mol) of the DFT[B3PW91]-calculated coordination energies.

From all these results, we believe that the CCSD(T) method with the FOC-QCP + SRC is useful to theoretically investigate the large transition metal complexes including *tert*-phosphine. However, the gradient has not been implemented at this moment and the SRC is not consistent with the geometry optimization. Also, the FOC-QCP parameters are not presented for various *tert*-phosphines such as PCy_3 (Cy = cyclohexyl), PPh_3, $POMe_3$, PF_3, and chelate diphosphine which are often used in many transition metal complexes. It is necessary to implement the gradient and to present parameters for various *tert*-phosphines.

Acknowledgment. This work was financially supported by Grant-in-Aids on basic research (No. 15350012), Priority Areas for "Molecular Theory for Real Systems" (No. 461), Creative Scientific Research, NAREGI project from the Ministry of Education, Science, Sports, and Culture, and Research Fellowships of the Japan Society for the Promotion of Science for Young Scientists. Some of the theoretical calculations were performed with PRIMEQUEST workstations of Institute for Molecular Science (Okazaki, Japan), and some of them were carried out with PC cluster computers of our laboratory.

Supporting Information Available: The complete form of ref 45. Cartesian coordinates of all species. This material is available free of charge via the Internet at http://pubs.acs.org.

References and Notes

(1) (a) Kameno, Y.; Ikeda, A.; Nakao, Y.; Sato, H.; Sakaki, S. *J. Phys. Chem. A* **2005**, *109*, 8055−8063. (b) Ikeda, A.; Nakao, Y.; Sato, H.; Sakaki, S. *J. Phys. Chem. A* **2007**, *111*, 7124−7132.

(2) (a) Kristyan, S.; Pulay, P. *Chem. Phys. Lett.* **1994**, *229*, 175−180. (b) Perez-Jorda, J. M.; Becke, A. D. *Chem. Phys. Lett.* **1995**, *233*, 134−137. (c) Zhang, Y.; Pan, W.; Yang, W. *J. Chem. Phys*. **1997**, *107*, 7921−

7925. (d) Tsuzuki, S.; Lüthi, H. P. *J. Chem. Phys*. **2001**, *114*, 3949−3957. (e) Wu, Q.; Yang, W. *J. Chem. Phys.* **2002**, *116*, 515−524.

(3) Sakaki, S.; Ohkubo, K. *J. Phys. Chem.* **1989**, *93*, 5655−5660.

(4) Ohnishi, Y.; Nakao, Y.; Sato, H.; Sakaki, S. *J. Phys. Chem. A* **2007**, *111*, 7915−7924.

(5) Brynda, M.; Gagliardi, L.; Widmark. P.-O.; Power, P. P.; Roos, B. O. *Angew. Chem., Int. Ed.* **2006**, *45*, 3804−3807.

(6) (a) Warshel, A. *Computer Modeling of Chemical Reactions in Enzymes and in Solutions*; Wiley: New York 1991. (b) Monard, G.; Merz, K. M., Jr. *Acc. Chem. Res.* **1999**, *32*, 904−911.

(7) Warshel, A.; Levitt, M. *J. Mol. Biol.* **1976**, *103*, 227−249.

(8) Singh, U. C.; Kollman, P. A. *J. Comput. Chem.* **1986**, *7*, 718−730.

(9) Field, M. L.; Bash, P. A.; Karplus, M. *J. Comput. Chem.* **1990**, *11*, 700−733.

(10) (a) McCammon, J. A.; Gelin, B. R.; Karplus, M. *Nature* **1977**, *267*, 585−590. (b) Karplus, M.; McCammon, J. A. *Nat. Struct. Biol.* **2002**, *9*, 646−652 and references therein.

(11) Sauer, J.; Sierka, M. *J. Comput. Chem.* **2000**, *21*, 1470−1493.

(12) Woo, T. K.; Margl, P. M.; Deng, L.; Cavallo, L.; Ziegler, T. *Catal. Today* **1999**, *50*, 479−500.

(13) (a) Maseras, F.; Morokuma, K. *J. Comput. Chem.* **1995**, *16*, 1170−1179. (b) Maseras, F. *Chem. Commun.* **2000**, 1821−1827. (c) Ujaque, G.; Maseras, F. *Struct. Bonding* **2004**, *112*, 117−150.

(14) Bakowies, D.; Thiel, W. *J. Phys. Chem.* **1996**, *100*, 10580−10594.

(15) Lyne, P. D.; Hadoscek, M.; Karplus, M. *J. Phys. Chem. A* **1999**, *103*, 3462−3471.

(16) Antes, I.; Thiel, W. *J. Phys. Chem. A* **1999**, *103*, 9290−9295.

(17) Eichinger, M.; Tavan, P.; Hutter, J.; Parrinello, M. *J. Chem. Phys.* **1999**, *110*, 10452−10467.

(18) Amara, P.; Field, M. J. *Theor. Chem. Acc.* **2003**, *109*, 43−52.

(19) Eurenius, K. P.; Chatfield, D. C.; Brooks, B. R.; Hodoscek, M. *Int. J. Quant. Chem.* **1996**, *60*, 1189−1200.

(20) Reuter, N.; Dejaegere, A.; Maigret, B.; Karplus, M. *J. Phys. Chem. A* **2000**, *104*, 1720−1735.

(21) Ferré, N.; Olivucci, M. *J. Mol. Struct. (THEOCHEM)* **2003**, *632*, 71−82.

(22) (a) Théry, V.; Rinaldi, D.; Rivail, J.-L.; Maigret, B.; Ferenczy, G. G. *J. Comput. Chem.* **1994**, *15*, 269−282. (b) Assfeld, X.; Rivail, J.-L. *Chem. Phys. Lett.* **1996**, *263*, 100−106. (c) Monard, G.; Loos, M.; Théry, V.; Baka, K.; Rivail, J.-L. *Int. J. Quantum Chem.* **1996**, *58*, 153−159. (d) Ferré, N.; Assfeld, X.; Rivail, J.-L. *J. Comput. Chem.* **2002**, *23*, 610−624.

(23) (a) Gao, J.; Amara, P.; Alhambra, C.; Field, M. J. *J. Phys. Chem. A* **1998**, *102*, 4714−4721. (b) Amara, P.; Field, M. J.; Alhambra, C.; Gao, J. *Theor. Chem. Acc.* **2000**, *104*, 336−343. (c) Garcia-Viloca, M.; Gao, J. *Theor. Chem. Acc.* **2004**, *111*, 280−286. (d) Pu, J.; Gao, J.; Truhlar, D. G. *J. Phys. Chem. A* **2004**, *108*, 632−650. (e) Pu, J.; Gao, J.; Truhlar, D. G. *J. Phys. Chem. A* **2004**, *108*, 5454−5463. (f) Pu, J.; Gao, J.; Truhlar, D. G. *Chem. Phys. Chem.* **2005**, *6*, 1853−1865.

(24) (a) Alhambra, C.; Corchado, J. C.; Sanchez, M. L.; Gao, J.; Truhlar, D. G. *J. Am. Chem. Soc.* **2000**, *122*, 8197−8203. (b) Alhambra, C.; Corchado, Sanchez, J. M. L.; Garcia-Viloca, M.; Gao, J.; Truhlar, D. G. *J. Phys. Chem. B* **2001**, *105*, 11326−11340. (c) Devi-Kesavan, L. S.; Gao, J. *J. Am. Chem. Soc.* **2003**, *125*, 1532−1540.

(25) (a) Humbel, S.; Siebar, S.; Morokuma, K. *J. Chem. Phys.* **1996**, *105*, 1959−1967. (b) Svenson, M.; Humbel, S.; Morokuma, K. *J. Chem. Phys.* **1996**, *105*, 3654−3661. (c) Svenson, M.; Humbel, S.; Froese, R. D. J.; Matsubara, T.; Siebar, S.; Morokuma, K. *J. Phys. Chem.* **1996**, *100*, 19357−19363. (d) Dapprich, S.; Komaromi, I.; Byun, K. S.; Morokuma, K.; Frisch, M. J. *J. Mol. Struct. (THEOCHEM)* **1999**, *461*−*462*, 1−21. (e) Vreven, T.; Morokuma, K. *J. Comput. Chem.* **2000**, *21*, 1419−1432.

(26) (a) Zhang, Y.; Lee, T.-S.; Yang, W. *J. Chem. Phys.* **1999**, *110*, 46−54. (b) Zhang, Y. *J. Chem. Phys.* **2005**, *122*, 024114.

(27) (a) DiLabio, G. A.; Hurley, M. M.; Christiansen, P. A. *J. Chem. Phys.* **2002**, *116*, 9578−9584. (b) Moon, S.; Christiansen, P. A.; DiLabio, G. A. *J. Chem. Phys.* **2004**, *120*, 9080−9086.

(28) Yasuda, K.; Yamaki, D. *J. Chem. Phys.* **2004**, *121*, 3964−3972.

(29) Slaviček, P.; Martínez, T. J. *J. Chem. Phys.* **2006**, *124*, 084107.

(30) (a) Alary, F.; Poteau, R.; Heully, J.-L.; Barthelat, J.-C.; Daudey, J.-P. *Theor. Chem. Acc.* **2000**, *104*, 174−178. (b) Poteau, R.; Ortega, I.; Alary, F.; Solis, A. R.; Barthelat, J.-C.; Daudey, J.-P. *J. Phys. Chem. A* **2001**, *105*, 198−205. (c) Bessac, F.; Alary, F.; Carissan, Y.; Heully, J.-L.; Daudey, J.-P.; Poteau, R. *J. Mol. Struct. (THEOCHEM)* **2003**, *632*, 43−59.

(31) Koga, N.; Morokuma, K. *Chem. Phys. Lett.* **1990**, *172*, 243−248.

(32) (a) Wang, K.; Rosini, G. P.; Nolan, S. P.; Goldman, A. S. *J. Am. Chem. Soc.* **1995**, *117*, 5082−5088. (b) Wang, K.; Goldman, A. S.; Li, C.; Nolan, S. P. *Organometallics* **1995**, *14*, 4010−4013.

(33) A common s/p set of even-tempered functions with exponents 0.12, 0.36, 1.08, 3.24, and 9.72. The d exponent is 0.626.

(34) Pacios, L. F.; Christiansen, P. A. *J. Chem. Phys.* **1985**, *82*, 2664−2671.

(35) Perdew, J. P.; Wang, Y. *Phys. Rev. B* **1992**, *45*, 13244−13249.

(36) Francl, M. M.; Petro, W. J.; Hehre, W. J.; Binkley, J. S.; Gordon, M. S.; DeFrees, D. J.; Pople, J. A. *J. Chem. Phys.* **1982**, *77*, 3654−3665.

(37) Hehre, W. J.; Ditchfield, R.; Pople, J. A. *J. Chem. Phys.* **1972**, *56*, 2257−2261.

(38) (a) Dunning, T. H., Jr. *J. Chem. Phys.* **1989**, *90*, 1007−1023. (b) Woon, D. E.; Dunning, T. H., Jr. *J. Chem. Phys.* **1993**, *98*, 1358−1371.

(39) Dolg, M.; Stoll, W. H.; Preuss, H. *J. Chem. Phys.* **1987**, *86*, 866−872.

(40) Andrae, D.; Haeussermann, U.; Dolg, M.; Stoll, H.; Preuss, H. *Theor. Chim. Acta* **1990**, *77*, 123−141.

(41) Frisch, M. J.; Pople, J. A.; Binkley, J. S. *J. Chem. Phys.* **1984**, *80*, 3265−3269.

(42) Martin, J. M. L.; Sundermann, A. *J. Chem. Phys.* **2001**, *114*, 3408−3420.

(43) Balabanov, N. B.; Peterson, K. A. *J. Chem. Phys.* **2005**, *123*, 064107.

(44) Cancés, M. T.; Mennucci, B.; Tomasi, J. *J. Chem. Phys.* **1997**, *107*, 3032−3041.

(45) Pople, J. A.; et al. *Gaussian03*, revision D.02; Gaussian, Inc.: Wallingford, CT, 2004.

(46) Chandler, J. P. Subroutine STEPIT—Finds local minima of a smooth function of several parameters. *Behav. Sci.* **1969**, *14*, 81−82.

(47) Chatt, J.; Shaw, B. L. *J. Chem. Soc.* **1959**, 705−716.

(48) Low, J. J.; Goddard, W. A., III. *J. Am. Chem. Soc.* **1986**, *108*, 6115−6128.

(49) Curtiss, L. A.; Raghavachari, K.; Trucks, G. W.; Pople, J. A. *J. Chem. Phys.* **1991**, *94*, 7221−7230.

(50) Matsubara, T.; Maseras, F.; Koga, N.; Morokuma, K. *J. Phys. Chem.* **1996**, *100*, 2573−2580.

(51) Svensson, M.; Humbel, S.; Froese, R. D. J.; Matsubara, T.; Sieber, S.; Morokuma, K. *J. Phys. Chem.* **1996**, *100*, 19357−19363.

(52) Though the SRC is effective for this size molecule, we wish to mention here that the SRC is still more time-consuming for a large system such as enzyme than the QM/MM method.

(53) (a) End-on coordination was proposed in the following: Thorn, D. L.; Tulip, T. H.; Ibers, J. A. *J. Chem. Soc., Dalton Trans.* **1979**, 2022−2025. (b) Side-on coordination was proposed in the following: Buesetto, C.; D'Alfonso, A.; Maspero, F.; Perego, G.; Zazzetta, A. *J. Chem. Soc., Dalton Trans.* **1977**, 1828−1834.

(54) Sakaki, S.; Morokuma, K.; Ohkubo, K. *J. Am. Chem. Soc.* **1985**, *107*, 2686−2693.